A lattice model Monte Carlo study of coil-to-globule and other conformational transitions of polymer, amphiphile, and solvent

Deirdre E. Jennings, Yuri A. Kuznetsov, Edward G. Timoshenko, and Kenneth A. Dawson[a)]
Department of Chemistry, University College Dublin, Belfield, Dublin 4, Ireland

(Received 26 March 1999; accepted 10 February 2000)

A model of polymer-amphiphile-solvent systems on a cubic lattice is used to investigate the phase diagram of such systems. The polymer is treated within the canonical ensemble $(T,V,\mathcal{N})$ and the amphiphile and solvent are treated within the grand canonical ensemble (T,V,μ). Using a range of Monte Carlo moves the phase diagram of polymer-amphiphile-solvent mixtures, as a function of solvent quality (parametrized by χ) and relative chemical potential, μ, is studied for the dilute polymer limit. The effect of increasing the polymer chain length, *N*, on the critical aggregation concentration (CAC), and the type of polymer-amphiphile complex formed above the CAC are also examined. For some parameters, it is found that the polymer and amphiphile form a polymer-micelle complex at low amphiphile concentrations, and that the polymer coil-to-globule transition point increases with increasing amphiphile concentration. The resulting collapsed globule has a solvent core and is surrounded by a layer of amphiphile. These results are in good qualitative agreement with experimental results for the poly(*N*-isopropylacrylamide) (PNIPAM)/sodium dodecyl sulfate (SDS) system. At higher amphiphile concentrations, the polymer and amphiphile form several layered structures depending on the strength of the three-body amphiphilic interactions, *l*. Finally, the effect of the polymer chain length, *N*, and the strength of the three-body amphiphilic interactions, *l*, on the stability of the polymer-amphiphile structures is investigated. © *2000 American Institute of Physics.* [S0021-9606(00)51817-0]

I. INTRODUCTION

The coil-to-globule transition of polymers has been extensively studied for many reasons and also as a simple model for protein folding. Theoretical investigations of Flory,[1] Huggins,[2] de Gennes[3–5] and many others[6–11] have shown that polymer conformation depends on solvent quality and other conditions such as temperature. In a good solvent the repulsive monomer–monomer interactions dominate and the polymer is a Flory coil. In a poor solvent attractive monomer–monomer interactions dominate and the polymer collapses and phase separates to a dilute phase of isolated collapsed globules and a concentrated phase of a polymer aggregates, though ultimately the actual situation depends on the experimental details. The coil-to-globule transition has been studied experimentally for a number of homopolymers including polystryene (PS), poly(*N*-isopropylacrylamide) (PNIPAM), and poly(*N*-isopropylmethylacrylamide) (PNIPMAM).[12–16] Computer simulations[17–22] have also been used extensively to study the different aspects of the transition and the properties of the coil and globule.

Experimentally, one is restricted to solutions of extremely dilute polymer concentrations when studying the coil-to-globule transition as phase aggregation is a problem. Amphiphiles increase the solubility of polymers and have been widely used to prevent aggregation in dilute polymer solutions. Schild and Tirrell[23,24] and Karlstrom *et al.*[25] have performed systematic studies of the effect of amphiphiles on the solubility of poly(*N*-isopropylacrylamide) (PNIPAM) and polyethyleneoxide (PEO), respectively. Recently, experimental and theoretical interest[26–37] has been focused on the coil-to-globule transition of polymers in the presence of amphiphile. It has been found that the critical temperature, at which a nonionic polymer, such as polyethyleneoxide (PEO) or poly(*N*-isopropylacrylamide) (PNIPAM) in aqueous solution undergoes the coil-to-globule transition, increases with increasing amphiphile concentration.[25,26]

In this paper, we begin by examining the dilute amphiphile regime for an isolated polymer chain. It is well known that amphiphiles bind to polymers to form mixed polymer-amphiphile aggregates at quite low amphiphile concentration (critical aggregation concentration, CAC). However, there has been much debate on the type of polymer-amphiphile complex formed at the critical aggregation concentration (CAC). There are two main models of the polymer-amphiphile mixed aggregate: the necklace model proposed by Cabane[38,39] where the polymer binds to the polar heads of a micelle in a ''loopy'' configuration, and the Kokufuto model[31] where the polymer backbone is incorporated into the core of the micelle. Walter *et al.*[26] proposed a third model for the poly(*N*-isopropylacrylamide) (PNIPAM)/sodium dodecyl sulfate (SDS) system where two types of micelles are formed: bound micelles where the polymer backbone is incorporated into the micelle core and quasi-free micelles. Using a hybrid Monte Carlo scheme, we examine the type of polymer-amphiphile complex formed at the CAC

a)Author to whom correspondence should be addressed.

and the effect of increasing the amphiphile concentration on the polymer coil-to-globule transition.

We have previously[40,41] investigated the types of polymer-amphiphile structures formed as a function of amphiphile concentration and amphiphilic strength. We have shown that the amphiphile self-assembles and incorporates the polymer into a variety of ''layered'' structures depending on the concentrations of polymer and amphiphile, the polymer chain length (N) and the strength of the three-body amphiphilic interactions ($l=L/k_BT$). Here, we investigate the regions of stability of the polymer-amphiphile structures as a function of solvent quality, χ. Throughout the paper we compared our results to the relevant experimental and theoretical results where possible.

II. MODEL AND METHOD

We model ternary mixtures of solvent (s), amphiphile (a) and polymer (m) on a lattice using a hybrid Monte Carlo scheme.[40] The solution is incompressible so that every site on the lattice is occupied. The total number of monomers (N_m) is constant as the degree of polymerization (N) and the number of polymer chains (M) are fixed. The polymer is therefore treated in a canonical ensemble $(T,V,\mathcal{N})$. The number of solvent and amphiphile molecules may vary and are treated in a grand canonical ensemble (T,V,μ). Our model for polymer-amphiphile-solvent mixtures is defined by the Hamiltonian

$$H_\mu \equiv H-\mu N_a, \tag{1}$$

$$H=-\sum_{\langle ij\rangle} w(r_{ij})I_{s_is_j}-\sum_{(ijk)} I_{s_is_js_k}, \tag{2}$$

where i, j, k enumerate the lattice sites, and s_i denotes the contents of the ith site. $I_{s_is_j}$ represents the two-body interactions where I_{mm}, I_{ms}, I_{ma}, I_{aa}, I_{ss}, I_{as} are the monomer–monomer, monomer–solvent, monomer–amphiphile, amphiphile–amphiphile, solvent–solvent, and amphiphile–solvent two-body interactions, respectively. The distance between sites i and j is denoted as $r_{ij}=|\vec{r}_i-\vec{r}_j|$. Short range interactions are introduced by the function $w(r_{ij})$ with the properties; $w(1b)=1$, $w(\sqrt{2}b)=1$, $w(\sqrt{3}b)=0.75$, $w(2b)=0.5$, and $w(r_{ij})=0$ for $r_{ij}>R_{\max}=2b$, where b is the unit spacing of the lattice. The linear three-body interaction parameter, $I_{s_is_js_k}$, can take on values of $+L$ for the favorable monomer–amphiphile–solvent (*mas*) interactions, $-L$ for the unfavorable monomer–amphiphile–monomer (*mam*), and solvent–amphiphile–solvent (*sas*) interactions and zero otherwise. Here $\mu=\mu_a-\mu_s$ is the relative chemical potential, where μ_a and μ_s are, respectively, the chemical potentials of the amphiphile and the solvent, and N_a is the number of amphiphile molecules.

There are several types of Monte Carlo moves used to update the system state. The creation and destruction of the solvent and amphiphile molecules is controlled by conventional Monte Carlo spin–flip type moves. There are two such moves: solvent to amphiphile ($s2a$) and amphiphile to solvent ($a2s$). Local internal moves and reptations are used to update the polymer conformation. Both use a special method, determined by the structure of the Hamiltonian, to generate neighborhood polymer structures while maintaining polymer connectivity and excluded volume constraints.[9,19] There are two types of elementary polymer moves: those involving the pairs monomer–solvent ($m2s$) and monomer–amphiphile ($m2a$).

The acceptance or rejection of a Monte Carlo move depends on the Metropolis ratio of transition probabilities, $\eta=\exp(-\Delta E/k_BT)$, where ΔE is the total change in energy between the final and initial states. It may be shown that the model depends only on the linear three-body interaction parameter, $I_{s_is_js_k}$, the relative chemical potential, μ, and on the following combinations of two-body interaction parameters $I_{s_is_j}$:

$$\chi_{m-m2s}=2I_{ms}-I_{mm}-I_{ss}, \tag{3}$$

$$\chi_{a-m2s}=I_{ms}+I_{as}-I_{ma}-I_{ss}, \tag{4}$$

$$\chi_{m-m2a}=I_{ms}+I_{ma}-I_{mm}-I_{as}, \tag{5}$$

$$\chi_{a-m2a}=I_{ms}+I_{aa}-I_{ma}-I_{as}, \tag{6}$$

$$\chi_{m-s2a}=I_{ms}-I_{ma}, \tag{7}$$

$$\chi_{a-s2a}=I_{as}-I_{aa}, \tag{8}$$

$$\chi_{s-s2a}=I_{ss}-I_{as}. \tag{9}$$

All interaction parameters are in units of k_BT, and we set $k_BT=1$.

We are interested in investigating the effect of changing the solvent quality from an good solvent to a poor solvent on the polymer conformation in the presence of amphiphile. A polymer is a Flory coil in an good solvent, due to the excluded volume interactions, and a collapsed globule in a poor solvent. Now we would like to study the collapse of the polymer chain to a globule in a solvent–amphiphile solution. Initially we set all the two-body interactions to zero and therefore all χ's in Eqs. (3)–(9) also reduce to zero. Setting the two-body interactions to zero models an ''athermal'' solvent in the Flory–Huggins theory.[1] The excluded volume constraints are explicitly included in our Monte Carlo scheme. Therefore, in this scheme, setting all two-body interactions equal to zero models a polymer in a good solvent.[9,19,40] To collapse the polymer we increase I_{ms} and I_{ma} simultaneously with all other two-body interactions set to zero. As I_{ms} and I_{ma} are increased it becomes more unfavorable for the monomers to interact with both the solvent and the amphiphile molecules and the polymer collapses to a globule in order to minimize the number of unfavorable monomer–solvent and monomer–amphiphile interactions.

Equations (3)–(9) then reduce to

$$\chi_{m-m2s}=2I_{ms}, \tag{10}$$

$$\chi_{m-m2a}=2I_{ma}, \tag{11}$$

$$\chi_{a-m2s}=\chi_{a-m2a}=0, \tag{12}$$

$$\chi_{m-s2a}=\chi_{a-s2a}=\chi_{s-s2a}=0. \tag{13}$$

The solubility of the polymer, χ, is defined here as $\chi = 2I_{ms} = 2I_{ma}$. As χ is increased it becomes more unfavorable for the monomers to interact with both the solvent and amphiphile molecules, and the polymer collapses to a globule. The value χ_c is defined as the point at which the polymer collapses to form a globule.

The Metropolis ratio of the transition probabilities for a monomer–solvent move (η_{m2s}), a monomer–amphiphile move (η_{m2a}), a solvent–amphiphile move (η_{s2a}), and a amphiphile–solvent move (η_{a2a}), now reduce to

$$\eta_{m2s} = \eta_{m2a} = \exp\left(\frac{\chi \Sigma_r w(r) \Delta n_m(r) - \Delta E_L}{k_B T}\right), \tag{14}$$

$$\eta_{s2a} = \exp\left(\frac{-\mu - \Delta E_L}{k_B T}\right), \tag{15}$$

$$\eta_{a2s} = \eta_{s2a}^{-1}, \tag{16}$$

where the summation is over all the neighboring sites with $w(r) > 0$, and $\Delta n_m(r)$ is the difference in the number of monomers between the final and initial states at each interaction distance, r. ΔE_L is the difference in the linear three-body interaction energy between the final and initial state, and μ is the relative chemical potential.

Obviously, the solubility of the polymer decreases as we increase χ. We know from the Flory theory for polymer–solvent mixtures that the transition point occurs at $\chi_c \simeq \frac{1}{2} + (1/\sqrt{N})$. However, though the scaling laws are universal, the exact location of the transition point is not universal and depends on the coordination number of the lattice. Our particular model is on a cubic lattice which takes into account interactions between nearest neighbors (6), diagonal neighbors (12), long diagonal neighbors (8) and next nearest neighbors (6). The transition point for our model occurs approximately at $\chi_c \simeq \frac{1}{4} + (1/\sqrt{N})$.

We are interested in the effect of the amphiphile presence on the solubility of the polymer. The linear three-body interaction parameter, $I_{s_i s_j s_k}$, is defined such that monomer–amphiphile–solvent interactions (I_{mas} or I_{sam}) have favorable energy ($+L$), whereas monomer–amphiphile–monomer interactions (I_{mam}) or solvent–amphiphile–solvent interactions (I_{sas}) have unfavorable energy ($-L$). All other linear three-body interactions are set to zero. This choice of interaction parameter reflects the direct tendency of the amphiphile to bind to the polymer and increase its solubility and the indirect tendency for the amphiphile to aggregate. This simple model may, in some respects, be viewed as the logical extension of the solvent–amphiphile lattice models that were studied a few years ago.[42–46] Here, as there, we aim to capture the essential energy scales, gross geometrical and computational features, but certainly not detailed properties. In particular, we know that lattices do distort geometries somewhat, and caution that subtle packing effects, which are not taken into account in this model, are often important. However, one should not over emphasize the limitations of lattice models. It has been found in solvent–amphiphile lattice models[47,48] that, above the roughening temperature of a model, the conformations and gross geometries are described reasonably well. Our feeling is that something similar pertains here and at least one should take some note of the general shape of the objects we describe. It would be unwise to make stronger statements than this about our prediction of geometry at the moment since in a sense we obtain ''model'' geometries.

III. RESULTS AND DISCUSSION

In the solvent rich phase we examine the binding of the amphiphile to a Flory coil and the effect of the amphiphile on the coil-to-globule transition on a polymer. We then examine the effect of decreasing the solubility of the polymer (increasing χ) on the conformation of the polymer–amphiphile aggregates in the more concentrated amphiphile regime. The investigations are made for lattice size, $S = 20$, and for an isolated polymer chain of length N. The monomer volume fraction is $\phi_m = MN/S^3$, where M is the number of polymer chains of length, N, and S^3 is the volume of the box. We focus on the very dilute limit, $M = 1$, to permit a clear discussion of the collapse of the polymer in the presence of amphiphile and polymer–amphiphile aggregation in the absence of interpolymer effects. The length of the polymer chain and lattice size are chosen to ensure that the polymer was long enough to clearly study the conformational transitions without any lattice size effects and yet is computationally efficient.

We exhibit results for a variety of values of the effective three-body interaction constant, $l = L/k_B T$, over a range of amphiphile–solvent concentrations and for $0 \leqslant \chi < 1.0$. The phase diagram is examined in three ways; by holding μ constant and changing χ, by holding χ constant and increasing μ, and finally by starting from a collapsed globule at different μ and decreasing χ. All simulations are run using preequilibrated initial configurations.

A. Investigation of the binding of the amphiphile to an isolated polymer and the type of polymer-amphiphile complex formed at the CAC (critical aggregation concentration)

We begin by looking at the binding of the amphiphile to a single polymer chain in a good solvent ($\chi = 0$) in the dilute amphiphile regime. Stauffer[49] defined the characteristic micelle concentration (CMC) as the concentration where half the amphiphile present is in the form of isolated particles and the other half is in the form of clusters consisting of two or more neighboring molecules. We use an analogous definition for the characteristic aggregation concentration of the amphiphile in the presence of polymer (CAC). We define μ_{CAC} and μ_{CMC} as the relative chemical potentials corresponding to the CAC and the CMC, respectively. Preliminary findings[41] for an isolated polymer of various chain lengths at $l = 1.0$, 1.66, 5.0 showed that the behavior of the CAC with increasing polymer chain length (N) and the type of polymer–amphiphile complex formed depend on the strength of the amphiphilic interactions (l). We investigate in greater detail the binding of the amphiphile to the polymer at the CAC for $N = 20$, 40, 80, 100, 120, 160 at $l = 1.0$, 1.66.

Figure 1 shows the plot of the ratio of the CAC to the CMC (CAC/CMC) versus N at $l = 1.0$, 1.66, 5.0. We note that the effect of increasing the polymer chain length (N) on

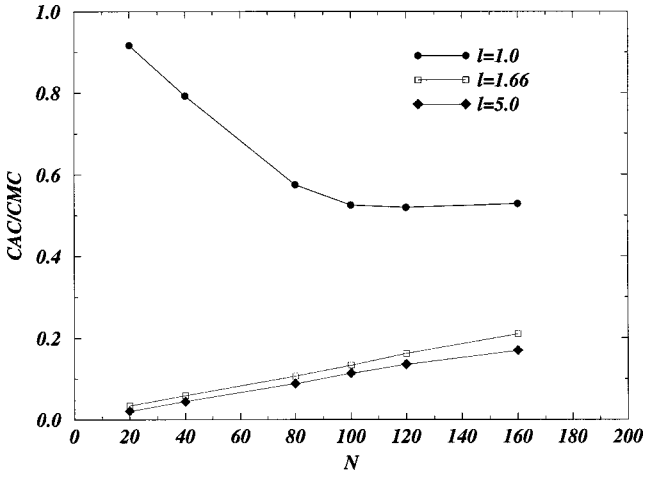

FIG. 1. Plot of the ratio of the CAC to the CMC (CAC/CMC), versus N at $l=1.0$ (○), $l=1.66$ (□), and $l=5.0$ (◇).

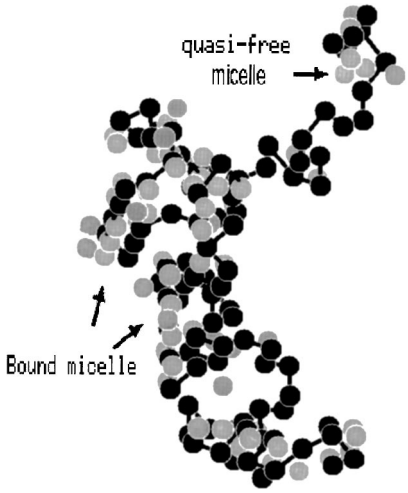

FIG. 2. Sample conformation of polymer–micelle complex formed above the critical aggregation concentration (CAC) for $N=100$ at $l=1.0$. Micelles are defined here as clusters of two or more neighboring amphiphiles. Bound micelles incorporate the backbone of the polymer chain into the core of the micelle and are associates with the polymer. The monomers are shown in black and the amphiphile in gray.

the CAC is completely different at $l=1.0$ and $l=1.66$, 5.0. For $l=1.66$ and $l=5.0$ the CAC/CMC increases linearly with N, whereas for $l=1.0$ the CAC/CMC decreases initially and then at a certain point ($N\approx 100$) is constant with increasing N. The effect of the polymer chain length on the critical aggregation concentration (CAC) at $l=1.0$ is in agreement with theoretical and experimental results.[25,26,50,51] For $l=1.0$, the strength of the amphiphilic interactions are comparable to k_BT, the isolated amphiphile is in solution and the polymer acts as a platform for forming clusters of amphiphile. As N increases the number of favorable (*mas*) interactions increase and therefore the amphiphiles form clusters more easily and the CAC decreases. However, for $N\geqslant 100$ the increase in the (*mas*) interactions is balanced by the fact that the amphiphile is now bound to a larger platform.

Examination of the configurations of the system for $N=100$ at $l=1.0$ show that isolated amphiphile molecules bind to the polymer before the onset of the cooperative association at the CAC. This indicates a strong hydrophobic interaction between the polymer and amphiphile. Above the CAC, we find that there are two types of polymer-bound micelles: the first type is where the polymer backbone is incorporated into the amphiphile cluster and the second type is where the amphiphile cluster is associated with the polymer. There are also free amphiphiles in solution. Figure 2 shows a sample conformation of the polymer–amphiphile complex formed above the CAC for $N=100$ at $l=1.0$. Finally, above the CMC the amphiphile forms unbound micelles in solution. Using our simple Monte Carlo hybrid scheme, we find that the binding of the amphiphile to the polymer and the type of polymer–amphiphile complex formed is similar to that proposed by Walter *et al.*[26] for the poly(*N*-isopropylacrylamide) and sodium dodecyl sulfate (PNIPAM–SDS) system.

The plots of the ratio CAC/CMC versus N for $l=1.66$ and $l=5.0$ are less typical of experimentally observed situations. At $l=1.66$, 5.0 the amphiphile binds to the polymer as soon as it is added to the system due to the strength of the favorable (*mas*) interactions and the unfavorable (*sas*) interactions (since $L>k_BT$). The CAC is then defined as the concentration where half the bound amphiphiles are in the form of isolated molecules and half the bound amphiphiles are in the form of clusters consisting of two or more neighboring amphiphiles. As N increases the number of monomers increases, therefore it is harder for the amphiphiles to form clusters and the CAC increases. Above the CAC the polymer–amphiphile forms a flat ''layered'' structure where the polymer is incorporated between two amphiphile monolayers in order to maximize the favorable (*mas*) interactions and minimize the unfavorable (*mam*) and (*sas*) interactions. Figure 3 shows a sample conformation of this *platelet* structure for $N=40$ at $l=1.66$.

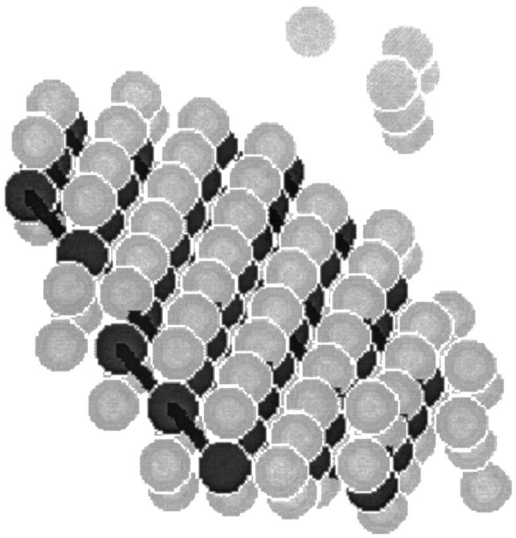

FIG. 3. Sample conformation of the collapsed polymer *platelet* structure formed beyond the CAC for $N=40$ at $l=1.66$. Solvent is represented as (white), amphiphile (gray), and polymer (dark gray/black).

In more concentrated amphiphile regimes a wide variety of structures are formed, from expanded coils to several different lamellar structures, depending on the polymer chain length (N), the strength of the amphiphilic interactions ($l = L/k_BT$) and the relative chemical potential (μ). Previously[40,41] we found that at $l=1.0$, for $N<80$ the polymer expands in the more concentrated amphiphile regimes to form an expanded coil, whereas for $N \geqslant 80$ the polymer and amphiphile collapses to an *interlayered sandwich* structure in the amphiphile rich regime and then re-expands to a coil in the amphiphile dense regime. For $l \geqslant 1.66$ the polymer collapses to a *platelet* structure above the CAC and in the amphiphile rich regime forms a series of *multilayered sandwich* structures where the number of layers increase with increasing amphiphile concentration. Finally, in the amphiphile dense regime the polymer re-expands to an expanded coil. Sample conformations of an *interlayered sandwich* structure ($N=100, l=1.0$) and a *multilayered sandwich* structure ($N=100, l=1.66$) are shown in Figs. (4a) and (4b), respectively.

B. Coil-to-globule transition of an isolated polymer chain in the presence of amphiphile

We now investigate the regions of existence of the polymer–amphiphile structures formed at $l=1.0$ and $l=1.66$ for $N=40$, 100 as a function of the solvent quality (χ) and relative chemical potential (μ). In investigating the phase diagram of a single polymer as a function of χ and μ we determine four broad regions of interest: the dilute amphiphile regime ($\mu<\mu_1$), the intermediate amphiphile regime ($\mu_1<\mu<\mu_2$), the more concentrated amphiphile regime ($\mu_2<\mu<\mu_3$), and the amphiphile dense regime ($\mu>\mu_3$). We find that in the dilute amphiphile regime ($\mu<\mu_1$) the transition points are self-consistent since, regardless of how we construct the partial phase diagram (by holding μ constant, varying χ, or by keeping χ constant, varying μ), they are fixed. This is a reassuring check on the simulation. However, for $\mu>\mu_1$, especially at $l=1.66$, we find that the polymer structures exhibit metastability as we increase χ.

We have shown that for $l=1.0$, at $\chi=0.0$ the behavior of the CAC with increasing polymer chain length, N, and the type of polymer-micelle complex formed above the CAC is in good qualitative agreement with experimental results. We investigate the effect of increasing the amphiphile concentration on the polymer coil-to-globule transition for $N=100$, at $l=1.0$. Figure 5 shows the phase diagram of the system for $N=100$ at $l=1.0$ as a function of χ and μ, where $\mu_{\mathrm{CAC}}=-2.65$, $\mu_1=\mu_{\mathrm{CMC}}=-1.6$, $\mu_2=0.6$, and $\mu_3=3.0$. We begin by examining the phase diagram for $N=100$, $l=1.0$ in the dilute amphiphile regime, $\mu<\mu_{\mathrm{CMC}}$. At very low amphiphile concentrations, $\mu<\mu_{\mathrm{CAC}}$, the coil-to-globule transition point, χ_c, increases slightly with increasing μ as amphiphile binds to the polymer and increases its solubility due to favorable (*mas*) interactions. This is in agreement with experimental and theoretical results.[25,26,36,37] Above the CAC the amphiphile binds to the polymer to form a mixed polymer–amphiphile aggregate and there is a dramatic increase in the χ_c value. χ_c increases linearly for $\mu>\mu_{\mathrm{CAC}}$ because the polymer–micelle complex is harder to collapse as it is stabilized by the favorable (*mas*) interactions and the unfavorable (*mam*) and (*sas*) interactions. During the coil-to-globule transition the mixed polymer–amphiphile aggregates undergo profound restructuring: solvent is enclosed in the globule due to the unfavorable (*mam*) interactions and amphiphile is bound to the outside of the globule due to the favorable (*mas*) interaction. Comparable observations are made in experimental work by Walter *et al.*[26] for PNIPAM–SDS system. Figure 6 shows sample conformations for $N=100$ at $l=1.0$ of a collapsed globule in the presence of amphiphile at (a) $\mu=-5.0$ (below the CAC) and (b) $\mu=-2.0$ (above the CAC).

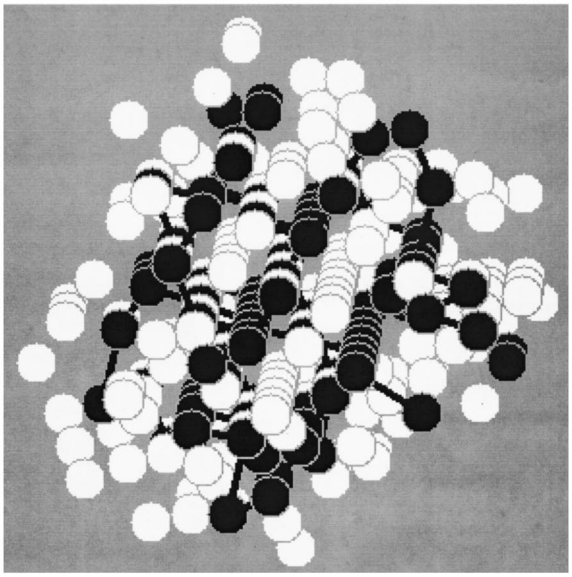
(a)

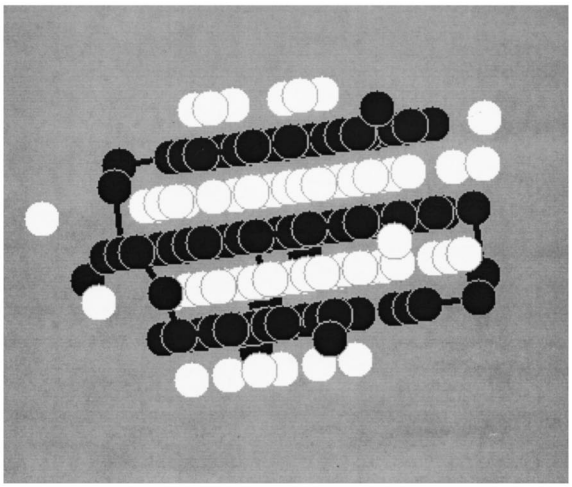
(b)

FIG. 4. Sample conformations of (a) an *interlayered sandwich* structure formed at $l=1.0$ and (b) a *multilayer sandwich* structure formed at $l=1.66$ for $N=100$ at $\chi=0.0$ in the amphiphile rich phase. For $N=100$ at $l=1.66$, $\chi=0.0$ the number of polymer layers in a sandwich structure increase from two (*bilayer*) to three or more (*multilayer*) with increasing μ. Polymer monomers are shown in black, with only the neighboring solvent molecules shown in white (up to next nearest neighbors). The amphiphile molecules are represented by a gray background.

Figure 7 shows the plot of the heat capacity, C_V/k_B, and the radius of gyration, R_g, versus χ, for $N=100$, $l=1.0$, at

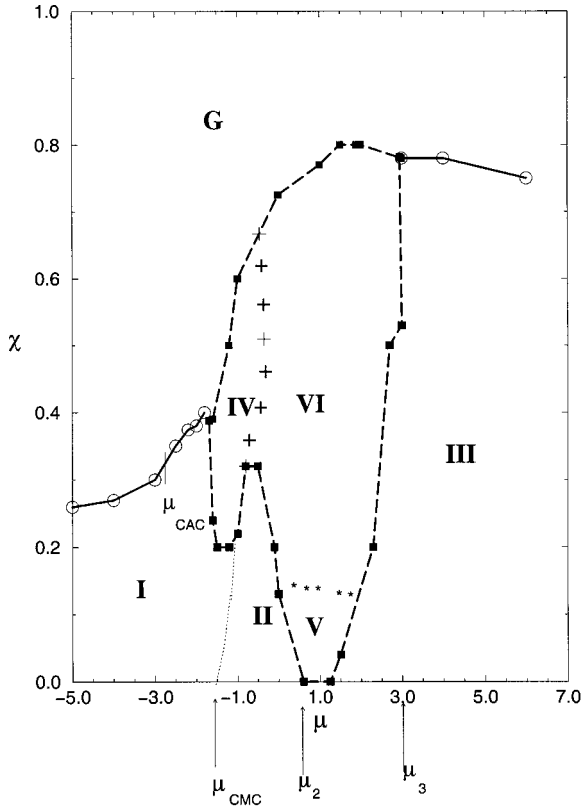

FIG. 5. The phase diagram for an isolated polymer of length $N=100$, is plotted for $l=1.0$ as a function of the relative chemical potential, μ, and the polymer solubility, χ. As μ increases the number of amphiphile molecules increase and the system goes from a solvent rich regime ($\mu<\mu_1$), to an intermediate amphiphile–solvent regime ($\mu_1<\mu<\mu_2$) to a more concentrated amphiphile regime ($\mu_2<\mu<\mu_3$) and finally to an amphiphile dense regime ($\mu>\mu_3$). $\mu_{CAC}=-2.65$, $\mu_1=\mu_{CMC}=-1.6$, $\mu_2=0.6$, and $\mu_3=3.0$, where μ_{CAC} and μ_{CMC} are the relative chemical potentials corresponding to the critical amphiphile concentration (CAC) and the critical micelle concentration (CMC), respectively. As χ increases the polymer solubility decreases and the polymer–amphiphile structures collapse to a globular structure. The regions of stability of the different polymer–amphiphile structures are I=Flory coil, II=overextended coil, III=expanded coil, IV=*platelet*, V=*interlayered sandwich* structure, VI=*multi-layered sandwich* structure, and G=collapsed globule. The thick solid lines with circles correspond to continuous transitions. Long-dashed lines with squares correspond to discontinuous transitions. The dotted line divides the region of stability of the Flory coil (I) and the overextended coil (II). The line of plus signs indicates the crossover from a *platelet* structure (IV) to *multilayer sandwich* structure (VI) and a line of stars indicates the crossover from the region of stability of the *interlayered sandwich* structure (V) and of the *multilayer sandwich* structures (VI).

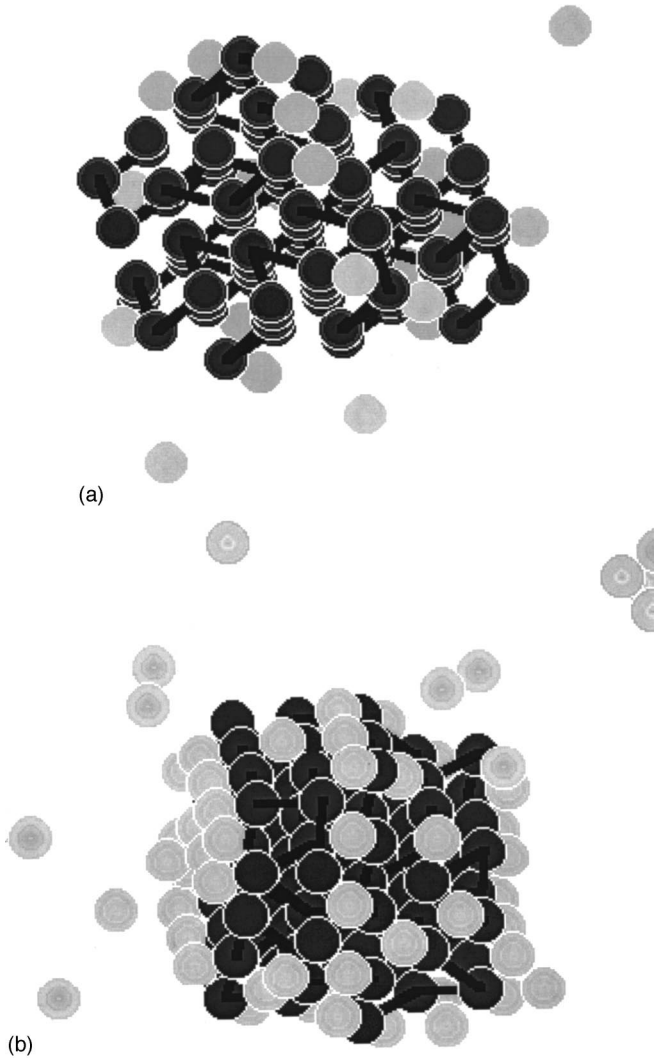

FIG. 6. Sample conformations for $N=100$, $l=1.0$ at (a) $\mu=-5.0$ and (b) $\mu=-2.0$ of a collapsed globule in the solvent rich phase. The monomers are shown in dark gray with black bonds and the amphiphiles are shown pale gray. The solvent molecules are not shown.

several different values of μ. We see a dramatic increase in the transition point and a broadening of the collapse transition with increasing $\mu(\mu>\mu_{CAC})$. This indicates that the amphiphile remains firmly associated with the polymer during the coil-to-globule transition. The increase in the transition temperature and broadening of the collapse transition with increasing amphiphile concentration has been observed experimentally by Walter *et al.*[26] for PNIPAM–SDS systems. It was also found experimentally that the polymer globules can be expanded to form coils by the addition of amphiphile. At $\chi=0.32$, we find that for $\mu>\mu_{CAC}$ the collapsed polymer globule expands to a restricted coil with increasing μ. Figure 8 shows a sample conformation of a restricted coil at $\mu=-1.8$ for $\chi=0.32$.

C. Conformational transitions of a single polymer chain, $N=100$, in the presence of amphiphile (amphiphilicity, $l=1.0$) as μ is increased, holding χ constant

We now examine in more detail the effect of increasing μ, while keeping χ constant, on the stability of the polymer–amphiphile structures. Figure 9 shows plots of the heat capacity, C_V/k_B and radius of gyration, R_g, versus μ, for $N=100$, $l=1.0$, at several different values of χ. For $N=100$, $l=1.0$ at $\chi=0.0$ there are three peaks in the heat capacity (B, B1, C). In the dilute amphiphile regime ($\mu<\mu_{CMC}$) the polymer chain is a Flory coil. As μ is increased further the system undergoes a solvent–amphiphile phase separation (peak B) and the polymer expands to an overextended coil. In the amphiphile rich phase, the polymer collapses from an overextended coil to form a polymer–amphiphile *interlay-*

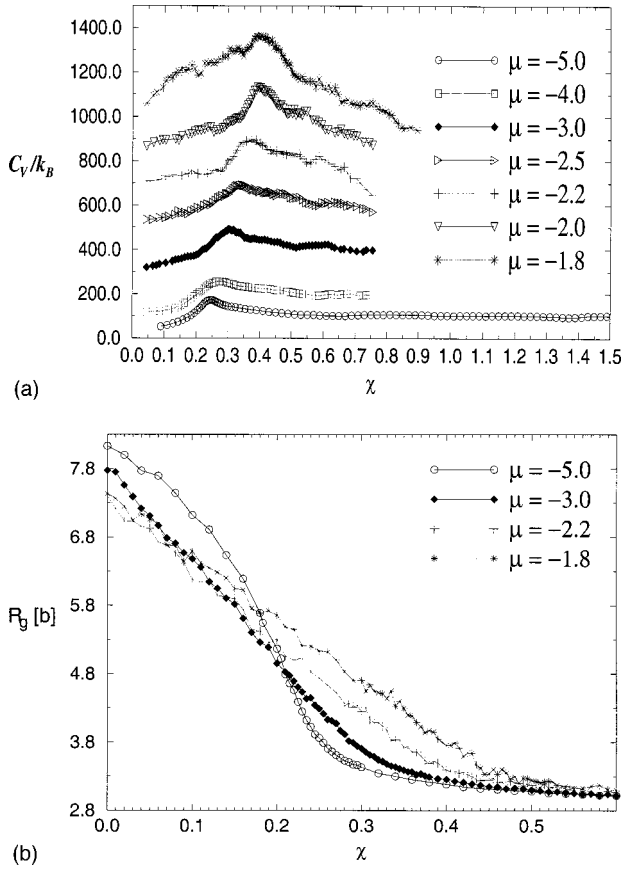

FIG. 7. (a) Plot of the running average of the heat capacity, C_V/k_B, versus χ, for $N=100$ at $l=1.0$ at different μ. Here $\mu=-5.0(\bigcirc)$, $\mu=-4.0(\square)$, $\mu=-3.0(\diamond)$, $\mu=-2.5(\triangleright)$, $\mu=-2.2(+)$, $\mu=-2.0(\triangledown)$, and $\mu=-1.8(\bigstar)$. (b) Plot of the radius of gyration, R_g, versus χ for $N=100$ at $l=1.0$ at $\mu=-5.0(\bigcirc)$, $\mu=-3.0(\diamond)$, $\mu=-2.2(+)$, and $\mu=-1.8(\bigstar)$. Note the behavior of the heat capacity, C_V/k_B, and the radius of gyration, R_g, versus χ changes above μ_{CAC}, the relative chemical potential corresponding to the critical aggregation concentration (CAC), where $\mu_{\mathrm{CAC}}\simeq -2.65$ for $N=100$ at $l=1.0$.

FIG. 8. A sample conformation of a restricted coil for $N=100$, $l=1.0$ in the solvent rich phase at $\mu=-1.8$, $\chi=0.32$. Only monomers (dark gray/black) and nearest neighboring amphiphile molecules (light gray) are represented.

ered sandwich structure [Fig. 4(a)] at peak B1 and then as μ increases further the polymer re-expands to form an expanded coil at peak C. For $\chi>0.0$, we will label the peak in the heat capacity corresponding to the collapse of the polymer from a coil-like structure to a *sandwich* structure peak B1* and the peak corresponding to the re-expansion of the polymer to a coil-like structure, peak C*.

At $\chi=0.32$ for $N=100$, $l=1.0$, the polymer is a collapsed globule in the very dilute amphiphile regime ($\mu<\mu_{\mathrm{CAC}}$). As μ increases the number of favorable (*mas*) interactions and unfavorable (*mam*), (*sas*) interactions increase and the polymer expands from a collapsed globule to a restricted coil. At $\mu\simeq\mu_{\mathrm{CMC}}$, the polymer undergoes what appears to be a discontinuous transition (peak R) from a restricted coil to a *platelet* structure to maximize the favorable (*mas*) interactions and minimize the unfavorable (*mam*) and (*sas*) interactions. As μ increases, the solvent and amphiphile phase separate and the polymer expands from a *platelet* to a coil-like structure at peak B. In the amphiphile rich phase, the polymer collapses from the coil-like structure to a *bilayer sandwich* structure at peak B1*. As μ increases further the number of solvent molecules decrease and the number of layers in the *sandwich* structure increases to maximize the favorable (*mas*) interactions. In the dense amphiphile region there is not enough solvent to stabilize the sandwich structure and the polymer expands to a coil at peak C*.

At $\chi=0.5$ we find that for $N=100$, $l=1.0$ the polymer is a collapsed globule in the dilute amphiphile region ($\mu<\mu_{\mathrm{CMC}}$). In the intermediate region, the number of amphiphiles increases rapidly with μ and the polymer expands from a globule to a *platelet* structure at peak V. Just after the solvent–amphiphile phase separation (peak B), the polymer rearranges from a *platelet* structure to a *bilayer* structure to maximize the favorable (*mas*) interactions. Finally, in the dense amphiphile regime the polymer re-expands to a coil-like structure at peak C*. For $\chi=0.8$ there are only two peaks in the heat capacity, B and Z. Peak B corresponds to the solvent–amphiphile phase separation. In the amphiphile rich phase it is harder to collapse the polymer because it is unfavorable to have amphiphile enclosed in the globule due to the unfavorable (*mam*) interactions. Peak Z corresponds to the region of stability of a *sandwich* structure where the three-body amphiphilic interactions (*mas, mam, sas*) briefly stabilize the *sandwich* structure. For $\chi>0.8$ there is only one peak in the heat capacity corresponding to the solvent–amphiphile phase separation and the polymer is a collapsed globule.

The observation of more *plateletlike* objects in some parts of the phase diagram could originate, in part, from the underlying lattice structure of this model. However, this is probably not the sole cause of the phenomenon which, we feel, is likely to have firm physical underpinnings. In the

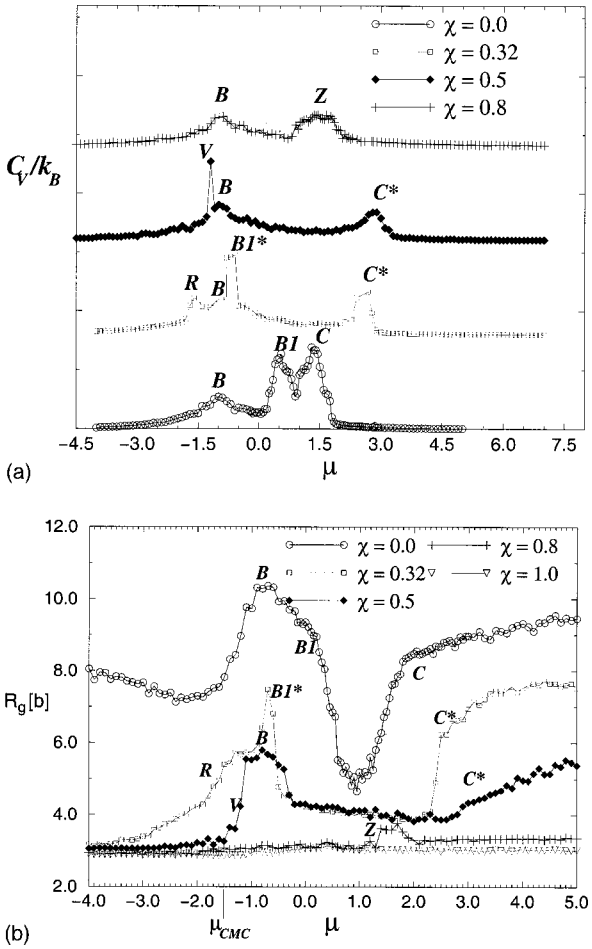

FIG. 9. (a) Plot of heat capacity, C_V/k_B, versus μ, for $N=100$, $l=1.0$ at $\chi=0.0(\bigcirc)$, $\chi=0.32(\square)$, $\chi=0.5(\diamond)$, and $\chi=0.8(+)$. (b) Plot of the radius of gyration, R_g, versus μ for $N=100$, $l=1.0$ at different χ. Here, $\chi=0.0(\bigcirc)$, $\chi=0.32(\square)$, $\chi=0.5(\diamond)$, $\chi=0.8(+)$, and $\chi=1.0(\triangledown)$. The peaks in the heat capacity and the corresponding changes in the radius of gyration of the polymer are labeled R, V, B, B1, B1*, C, C*, and Z to facilitate discussion in the text.

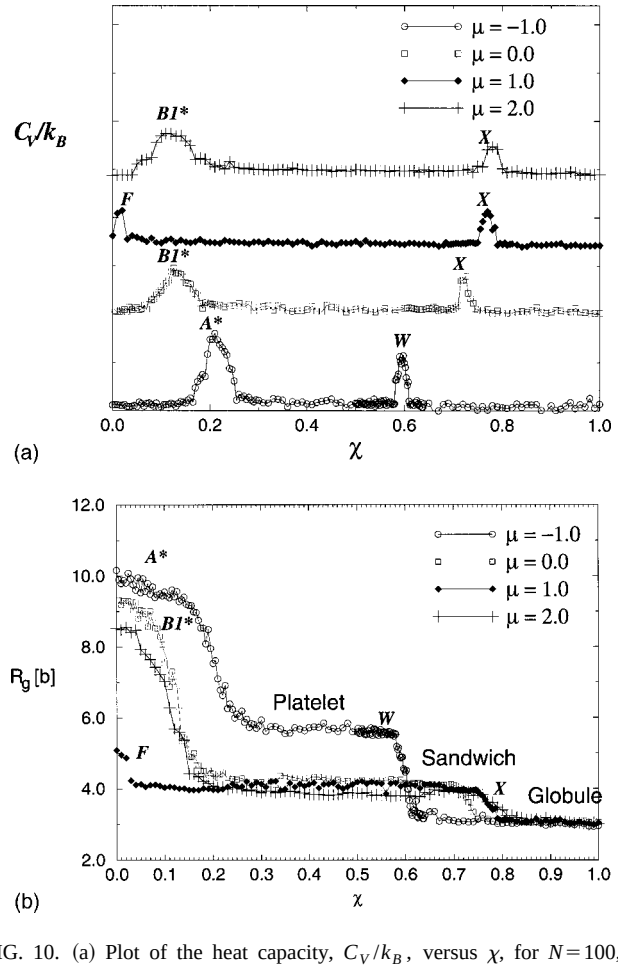

FIG. 10. (a) Plot of the heat capacity, C_V/k_B, versus χ, for $N=100$, $l=1.0$ at fixed μ. (b) Plot of the radius of gyration, R_g, versus χ, for $N=100$, $l=1.0$ at different μ. Here $\mu=-1.0(\bigcirc)$, $\mu=0.0(\square)$, $\mu=1.0(\diamond)$, $\mu=2.0(+)$. The peaks in the heat capacity and the corresponding changes in the radius of gyration of the polymer are labeled F, B1*, A*, W, and X to facilitate discussion in the text.

absence of polymer, parts of the phase diagram are dominated by lamellar amphiphile states. These originate in the microscopic interactions that produce a curvature energy. The presence of polymer we argue, shifts this tendency in the parameter space, and it is likely that in some systems flattened micellar objects do associate with polymers. The role of the lattice is likely to overemphasize these natural effects.

D. Conformational transitions of a single polymer chain, $N=100$, in the presence of amphiphile (amphiphilicity, $l=1.0$) as χ is increased, holding μ constant

We now investigate the effect of decreasing the polymer solubility, i.e., increasing χ, on the stability of the polymer–amphiphile structures for $\mu>\mu_{\mathrm{CMC}}$. We examine the plots of the heat capacity, C_V/k_B, and radius of gyration, R_g, versus χ for $N=100$ at $l=1.0$ in the intermediate amphiphile regime at $\mu=-1.0$ (solvent rich phase) and $\mu=0.0$ (amphiphile rich phase), and in the more concentrated amphiphile regime at $\mu=1.0$ and $\mu=2.0$ (Fig. 10). We begin by looking at the intermediate amphiphile regime, $-1.6<\mu<0.6$, where at $\chi=0.0$ the polymer is an overextended coil. At $\mu=-1.0$ there are two peaks in the heat capacity: peak A* which corresponds to the conformational transition from an overextended coil to a *platelet* structure, and peak W which corresponds to the collapse of the polymer from a *platelet* to a globule. The peak corresponding to collapse of the polymer from an overextended coil to a *platelet* structure is labeled A* as a similar coil-to-platelet transition occurs at $\chi=0.0$ with increasing μ at $l=1.66$. As χ increases, the polymer tries to minimize the number of unfavorable two-body monomer–solvent (m–s) and monomer–amphiphile (m–a) interactions. However, the linear three-body amphiphilic interactions (*mas*), (*mam*), and (*sas*) cause the polymer to initially collapse to a *platelet* structure as this maximizes the favorable (*mas*) interactions while minimizing the unfavorable ($m-a$), ($m-s$), (*mam*), and (*sas*) interactions. As χ increases further the unfavorable two-body $m-a$, $m-s$ interactions outweigh the linear three-body amphiphilic interactions stabilizing the *platelet* structure and the polymer collapses to form a globule. At $\chi=0.0$ the polymer expands with increasing μ to an overextended coil in the amphiphile rich phase ($\mu\geqslant 0.0$). At $\mu=0.0$ we find that as χ increases

the polymer undergoes two discontinuous transitions: from an overextended coil to a *bilayer sandwich* structure at peak B1* and from the *bilayer* to a collapsed globule at peak X. At higher μ, peak X corresponds to the collapse of an *interlayered/multilayered sandwich* structure to a globule. The polymer collapses with increasing χ in order to minimize the unfavorable two-body monomer–solvent and monomer–amphiphile interactions while maximizing the favorable (*mas*) interactions. The transition point at which these ''intermediate'' polymer–amphiphile structures collapse to a globule increases with increasing μ due to the increase in the number of favorable (*mas*) and unfavorable (*mam*) interactions.

We now examine the more concentrated amphiphile region, $\mu_2<\mu<\mu_3$, for $N=100$ at $l=1.0$ where $\mu_2=0.6$ and $\mu_3=3.0$. At $\chi=0.0$, the polymer is an *interlayered sandwich* structure for $0.6<\mu<1.4$ and an expanded coil for $\mu>1.4$. We find that as χ increases, regardless of the initial polymer structure the polymer collapses first to a *multilayered sandwich* structure and then to a globule. Figure 10 shows sample plots of the heat capacity and radius of gyration versus χ for $\mu=1.0(\diamond)$, where the polymer is an *interlayered sandwich* at $\chi=0.0$, and for $\mu=2.0(+)$, where the polymer is an expanded coil at $\chi=0.0$. At $\mu=1.0$ as χ increases there are two peaks in the heat capacity; peak F and peak X. Peak F corresponds to the collapse of the polymer from an *interlayered sandwich* structure to a *multilayered sandwich* and occurs at very low χ. Peak X occurs at much higher χ and corresponds to the conformational transition from a *multilayered sandwich* to a globule. At $\mu=2.0$, as χ increases the polymer collapses initially from an expanded coil to a *multilayered sandwich* at peak B1* and then to a collapsed globule at peak X. The *multilayered sandwich* polymer–amphiphile structure collapses with increasing χ to minimize the unfavorable monomer–solvent interactions while maximizing the favorable (*mas*) interactions. As μ increases the number of layers in a *multilayered sandwich* structure increase, and the sandwich-to-globule transition point increases as it becomes harder to rearrange the amphiphile so it is excluded from the center of the globule.

In the dense amphiphile phase ($\mu>\mu_3$), as χ increases the polymer undergoes a continuous transition from an expanded coil to a globule. This is similar to the coil-to-globule transition in the solvent rich phase. However, in the dense amphiphile regime there is very little solvent present so the polymer globule contains amphiphile in the center which results in unfavorable (*mam*) interactions. It is harder to collapse the polymer to a globule in the dense amphiphile regime than in the solvent rich regime due to the unfavorable (*mam*) interactions. The transition point decreases only slightly with increasing μ, as the decrease in the number of (*mas*) interactions stabilizing the expanded coil is counterbalanced by the increase in the number of (*mam*) interactions destabilizing the globule. The collapse transition is much broader in the dense amphiphile regime as it is very hard to collapse the polymer from a swollen globule to a completely collapsed globule due to the unfavorable (*mam*) interactions.

E. Investigating the effect of changing the polymer chain length, *N*, and the strength of the three-body amphiphilic interactions, $l=L/k_BT$, on the phase diagram of the system

We now compare the phase diagram for $N=100$ at $l=1.0$ as a function of χ and μ and the phase diagrams for $N=40$, $l=1.0$ (Fig. 11) and $N=100$, $l=1.66$ (Fig. 12) to see the effect of the polymer chain length, and the strength of the amphiphilic interactions on the phase diagram. We note that the phase diagrams at $l=1.0$ for $N=40$ and $N=100$ are very similar. For $N=40$ at $l=1.0$ the polymer undergoes a continuous transition from a Flory coil to a collapsed globule in the dilute amphiphile regime. Comparison of the transition points for $N=40$ and $N=100$ at the $\mu=-5.0$ shows that χ_c decreases with increasing N, which is the same as for pure polymer–solvent mixtures $[\chi_c\propto(1/\sqrt{N})]$[1]. Here χ_c for $N=40$, $l=1.0$ also increases for $\mu_{CAC}<\mu<\mu_{CMC}$ but not as dramatically as for $N=100$. For $N=40$, $l=1.0$ at $\chi=0.0$, as μ increases ($\mu>\mu_{CMC}$) the polymer expands to an over extended coil during the solvent–amphiphile phase separation and then collapses to an expanded coil. In the intermediate amphiphile regime ($\mu_{CMC}<\mu<\mu_2$), as χ is increased the polymer undergoes discontinuous transitions. The polymer initially collapses from an overextended coil to a *platelet* in the solvent rich phase or a *sandwich* structure in the amphiphile rich phase and then collapses to a globule. The crossover from *platelet* to *sandwich* structure shifts to lower μ with increasing χ. This is to be expected as the *sandwich* structure is more stable than the *platelet* as it has more favorable (*mas*) interactions. The region of stability of these ''layered'' structures for $N=40$ is much narrower than for $N=100$ due to the shorter chain length [fewer favorable (*mas*) and unfavorable (*mam*) interactions]. In the more concentrated amphiphile regime, the collapse from the expanded coil to a globule also occurs at lower χ for $N=40$ than for $N=100$ due to smaller number of (*mas*) interactions stabilizing the coil. We find that as N increases the region of stability of the polymer–amphiphile structures increase and it is harder to collapse the polymer to a globule, especially in the amphiphile rich phase.

We sketch the phase diagram for $N=100$ at $l=1.66$ as a function of μ and χ (Fig. 12), where $\mu_{CAC}=-3.8$, $\mu_1=-0.5$, $\mu_2=0.6$, and $\mu_3=7.0$. At $l=1.66$ the amphiphilic (*mam, sas, mas*) interactions are very strong which means that the amphiphile binds to the polymer as soon as it is added to solution and the amphiphile monolayer does not want to bend. At $\chi=0.0$, for $N=100$, $l=1.66$ the polymer is a Flory coil in the very dilute amphiphile regime ($\mu<\mu_{CAC}$). As μ increases the polymer collapses to a *platelet* structure and this may be rationalized as reducing the effective bending energy of the amphiphile monolayer. The *platelet* is stable in the solvent rich phase for $\mu>\mu_{CAC}$ as this flat ''layered'' structure maximizes the favorable (*mas*) interactions and minimizes the unfavorable (*mam*) and (*sas*) interactions. As the system undergoes the solvent–amphiphile phase separation the *platelet* structure expands initially and then collapses in the amphiphile rich phase to a *bilayer sandwich* structure. As μ increases the number of solvent molecules decreases, and in order to maximize the favorable

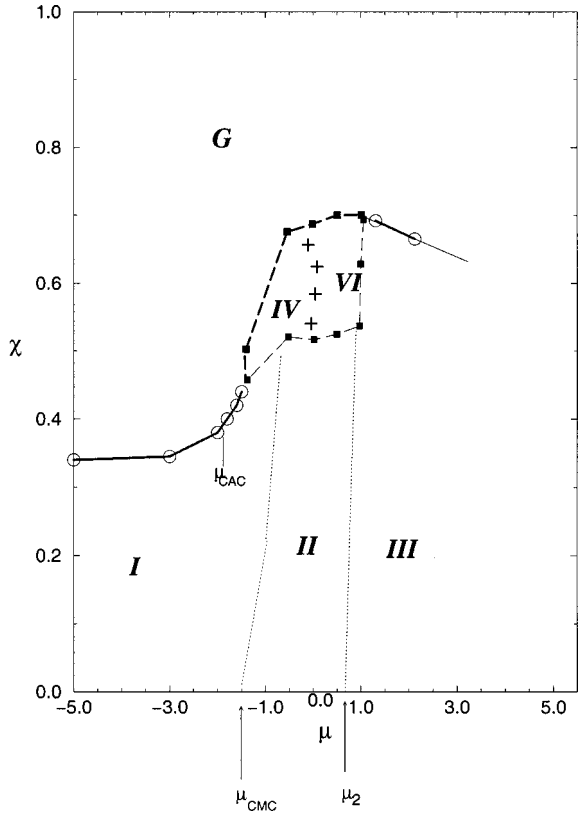

FIG. 11. The phase diagram for $N=40$ at $l=1.0$ is plotted as a function of μ and χ. As μ, the relative chemical potential, increases the number of amphiphile molecules increase and the system goes from a solvent rich regime ($\mu<\mu_1$), to an intermediate amphiphile–solvent regime ($\mu_1<\mu<\mu_2$), to an amphiphile-rich regime ($\mu>\mu_2$). $\mu_{CAC}=-1.75$, $\mu_1=-1.5$, and $\mu_2=0.7$. As χ increases the polymer solubility decreases and the polymer–amphiphile structures collapse to a globular structure. The regions of stability of the different polymer–amphiphile structures are I=Flory coil, II=overextended coil, III=expanded coil, IV=*platelet*, VI=*sandwich* structure, and G=collapsed globule. The thick solid lines with circles correspond to continuous transitions. Long-dashed lines with squares correspond to discontinuous transitions. The dotted line divides the regions of stability of the Flory coil (I), the overextended coil (II), and expanded coil (III). The line of plus signs indicates the crossover from a *platelet* structure (IV) to *sandwich* structures (VI). This crossover is not sharp and shifts with increasing χ to lower μ.

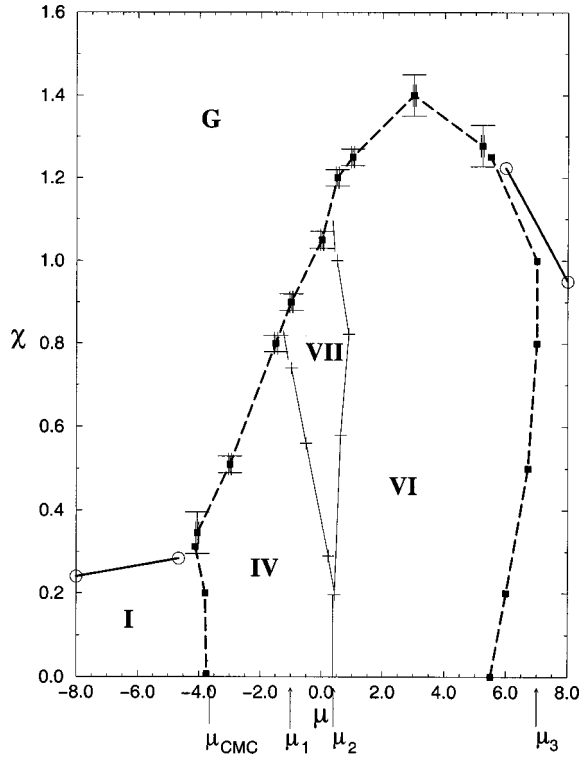

FIG. 12. The phase diagram for $N=100$ at $l=1.66$ plotted as a function of μ and χ. As μ, the relative chemical potential, increases the number of amphiphile molecules increase and the system goes from a solvent rich regime ($\mu<\mu_1$), to an intermediate amphiphile–solvent regime ($\mu_1<\mu<\mu_2$), to a more concentrated amphiphile regime ($\mu_2<\mu<\mu_3$), and finally to the amphiphile dense regime ($\mu>\mu_3$). $\mu_{CAC}\simeq-3.5$, $\mu_1=-1.0$, $\mu_2=0.4$, and $\mu_3=7.0$. As χ increases the polymer solubility decreases and the polymer–amphiphile structures collapse to a globular structure. The regions of stability of the different polymer–amphiphile structures are I=Flory coil, II=overextended coil, III=expanded coil, IV=*platelet*, VI=*multilayer sandwich* structure, VII=*platelet* and *sandwich* structures, and G=collapsed globule. Region VII is denoted by solid lines with plus marks (+) and corresponds to where both the *platelet* and *sandwich* structures coexist. The thick solid lines with circles correspond to continuous transitions. Long-dashed lines with squares and error bars correspond to discontinuous transitions. Error bars are shown for the discontinuous transition from layered polymer–amphiphile structures to collapsed globule.

(*mas*) interactions the number of layers in a *sandwich* structure increases. Finally, in the dense amphiphile regime there is not enough solvent to stabilize these ''layered'' structures and the polymer expands to an expanded coil.

At $\chi=0.0$ for $N=100$, $l=1.66$, the polymer is a Flory coil in the very dilute amphiphile phase. As χ is increased the polymer undergoes a continuous transition to a collapsed globule. In the dilute amphiphile regime ($\mu<\mu_{CAC}$), there is very little amphiphile present and we find that the coil-to-globule transition occurs at the same χ_c as for $N=100$ at $l=1.0$. For $\mu_{CAC}<\mu<\mu_3$, the preferred structure of the polymer–amphiphile aggregates is a flat ''layered'' structure. As χ increases, the two-body monomer–amphiphile $(m-a)$ and monomer–solvent $(m-s)$ interactions become more unfavorable and the polymer collapses to try to minimize the monomer–amphiphile and monomer–solvent contacts. The three-body amphiphilic interaction makes long straight pieces of chain more favorable, while the two-body $(m-s)$, $(m-a)$ interactions cause compaction. We find at $l=1.66$, that as χ increases the polymer–amphiphile ''layered'' structures collapse to form a flatter more ordered globule than at $l=1.0$. Figure 13 shows a sample conformation of the collapsed globule for $N=100$, $l=1.66$ at $\mu=-1.0$. This globule structure is similar to the orientationally ordered globules found by Kuznetsov *et al.*[52] for homopolymers in pure solvent with two-body and three-body interactions. At $l=1.66$, the *platelet*-to-*globule* and *sandwich*-to-*globule* transitions occur at much higher χ than for $l=1.0$. If we hold μ constant and increase χ, we find that the *platelet* and *sandwich* structures collapse to a globule through a series of layered structures such as those shown in Fig. 14. The intermediate collapse structures are a compromise between minimizing the bending of the amphiphile monolayer [maximizing favorable (*mas*) interactions] and maximizing the compaction (minimizing unfavorable monomer–solvent and monomer–amphiphile interactions). In the solvent rich phase the intermediate collapse structure is a flat globule consisting

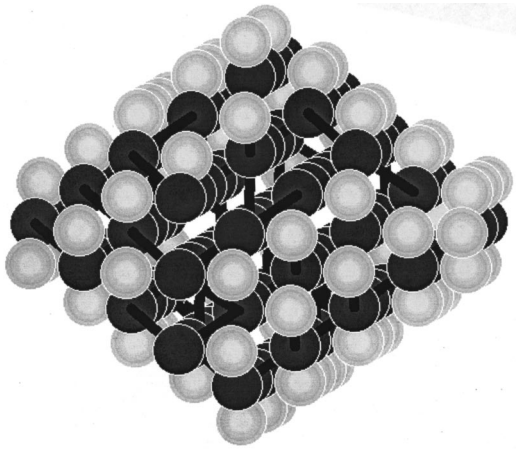

FIG. 13. A sample conformation of a collapsed globule for $N=100$, $l=1.66$ at $\mu=-2.0$. Only monomers (dark gray/black) and nearest neighboring amphiphile molecules (light gray) are represented.

of a layer of monomer–solvent–monomer molecules between two amphiphile monolayers and surrounded by solvent [Fig. 14(a)]. In the amphiphile rich phase the intermediate collapse structure is between a *sandwich* structure and a globule [Fig. 14(b)]. We note that in the intermediate amphiphile region ($\mu_1<\mu<\mu_2$) the *platelet* and *sandwich* structures coexist. This region of co-existence increases with increasing χ. In the dense amphiphile regime ($\mu>\mu_3$), the polymer is a expanded coil at $\chi=0.0$. The collapse transition from an expanded coil to a globule in the amphiphile rich regime occurs at higher χ_c for $l=1.66$ than for $l=1.0$ due to the increased strength of the unfavorable (*mam*) interactions which inhibit collapse.

IV. CONCLUSION

In this paper we have extended our earlier work to investigate the stable phases and structure of the phase diagram for polymer–amphiphile–solvent mixtures. However, as yet we are able to study only relatively dilute polymer solutions. Also, in the dilute polymer and amphiphile regime, we investigate the effect of the polymer on the CMC (critical micelle concentration), the type of polymer–amphiphile complex formed, and the effect of the amphiphile on the collapse transition of the polymer. We find that for $l=1.0$ the behavior of the CAC with increasing polymer chain length and the type of polymer–micelle complex formed is in good qualitative agreement with theoretical and experimental results.[25,26,50,51]

First, we have investigated the effect of increasing the amphiphile concentration on the polymer coil-to-globule transition. For $N=100$ at $l=1.0$, we find that in the dilute amphiphile regime ($\mu<\mu_{\mathrm{CMC}}$) as χ increases the polymer undergoes a continuous transition from a Flory coil to a collapsed globule. We find that above the CAC the polymer collapses to a globule surrounded by a layer of amphiphile, and that the transition point, χ_c, increases dramatically with increasing the amphiphile concentration. We also find that for $N=100$ at $l=1.0$ the collapsed globule can be expanded by adding more amphiphile. These results are in good qualitative agreement with those found experimentally by Walter *et al.*[26] for a poly(*N*-isopropylacrylamide) and sodium dodecyl sulfate (PNIPAM–SDS) system in aqueous solution.

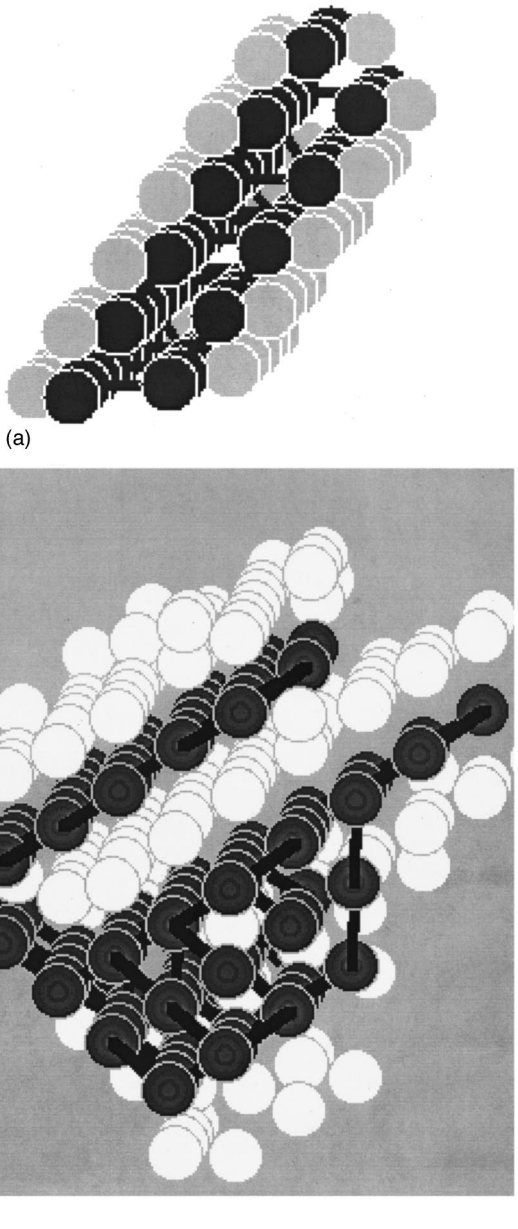

FIG. 14. Sample conformations of a semicollapsed globule for $N=100$, $l=1.66$ in (a) the solvent rich phase at $\mu=-3.0$ and (b) the amphiphile rich phase at $\mu=2.0$. In the solvent rich phase [$\mu=-3.0$(a)] the monomers (dark gray/black) and nearest neighboring amphiphile molecules (light gray) are shown on a white background which represents the solvent. In the amphiphile rich phase [$\mu=2.0$(b)] the monomer (dark gray/black) and the next nearest neighboring solvent molecules (white) are shown on a light gray background which represents the amphiphiles.

Second, we have examined the effect of changing the solvent quality (parameterized by χ) on the stability of the polymer–amphiphile structures in the dilute polymer limit. For $N=100$, $l=1.0$ in the intermediate amphiphile regime, $\mu>\mu_{\mathrm{CMC}}$, as χ increases the polymer collapses initially to a ''layered'' polymer–amphiphile structure and then to a globule, both of which are discontinuous transitions. The number of ''layers'' in the polymer–amphiphile structure increases

with increasing μ, from a *platelet* structure (one layer), to a *bilayer sandwich* structure (two layers) to a *multilayered sandwich* (three/four/five layers). We know of no current experimental data to confirm our observations about these flattened micellar structures. The transition point corresponding to the collapse of a ''layered'' structure to a globule increases with increasing μ due to the increase in the number of amphiphilic (*mas, mam, sas*) interactions stabilizing the structure. In the very dense amphiphile regime the polymer again undergoes a discontinuous transition from an expanded coil to a globule. In this regime, there is amphiphile is in the center of the globule, which is unfavorable due to the unfavorable (*mam*) interactions and results in a very broad collapse transition.

Third, we have also investigated the effect of decreasing the polymer chain length (N) and increasing the strength of the amphiphilic interactions (l) on the polymer–amphiphile–solvent phase diagram. Comparison of the phase diagram for $N=40$ and $N=100$ at $l=1.0$ shows that, in the very dilute amphiphile regime, the coil-to-globule transition point increases with decreasing N. This is the same as for pure polymer–solvent mixture. At $l=1.0$ we find that for $N=40$ the coil-to-globule transition point increases above μ_{CAC} but not as dramatically as for $N=100$. In the more concentrated amphiphile regime, the stability of the polymer–amphiphile ''layered'' structures increases with increasing N due to the increased number of (*mas*) and (*mam*) interactions. In the dense amphiphile phase, the transition point corresponding to the collapse of an expanded coil to a globule increases in χ with increasing N. Comparison of the phase diagrams for $N=100$ at $l=1.0$ and $l=1.66$ shows that as l increases the stability of the polymer–amphiphile ''layered'' structures increases dramatically. At $l=1.66$, it is much harder to collapse the polymer–amphiphile ''layered'' structures and the expanded coil to a globule. Also at $l=1.66$ the structure of the globule is flatter and more ordered as it is harder to bend the amphiphile monolayer at higher values of l.

To conclude, in this paper we have extended previous work and begun to explore, albeit in a schematic way, the phase behavior of polymer–amphiphile–solvent systems using Monte Carlo simulation. We realize that there are limitations present in our simulation. Amongst these is an overestimation of the sharpness of polymer coil-to-globule transition due to crystallization effects and other lattice-induced effects and the fact that we do not take into account packing effects on the geometry of the polymer–amphiphile structures. However, we do not expect the limitations to be reflected in any more serious manner in the polymer–amphiphile–solvent system studied here than in the established two and three component amphiphile systems. We have found that, for some parameters, we have good qualitative agreement with experiment. For other parameters, we find novel structures, which may yet be observed in experiment.

[1] P. J. Flory, *Principles of Polymer Chemistry* (Cornell University Press, Ithaca, NY, 1953), Chap. XIII.
[2] M. L. Huggins, J. Phys. Chem. **46**, 151 (1942).
[3] P. G. de Gennes, *Scaling Concepts in Polymer Physics*, 3rd ed. (Cornell University Press Ithaca, New York, 1988).
[4] P. G. de Gennes, J. Phys. (France) Lett. **36**, L55 (1975).
[5] P. G. de Gennes, J. Phys. (France) Lett. **39**, L299 (1978).
[6] J. des Cloiseaux and G. Jannix, *Polymers in Solution* (Oxford University Press, Walton Street, Oxford OX2 6DP, 1989).
[7] B. J. Cherayil, J. F. Douglas, and K. F. Freed, J. Chem. Phys. **83**, 5293 (1985).
[8] A. Y. Grosberg and D. V. Kuznetsov, Macromolecules **25**, 1970 (1992); , 1980 (1992); , 1991 (1992); , 1996 (1992).
[9] A. Y. Grosberg and A. R. Khokhlov, *Statistical Physics of Macromolecules* (AIP Press, New York, 1994).
[10] Y. A. Kuznetsov, E. G. Timoshenko, and K. A. Dawson, J. Chem. Phys. **104**, 3338 (1996).
[11] E. G. Timoshenko, Y. A. Kuznetsov, and K. A. Dawson, Phys. Rev. E **53**, 3886 (1996).
[12] T. Binkert, J. Oberreich, M. Meewes, R. Nyffenegger, and J. Rička, Macromolecules **24**, 5806 (1991).
[13] E. I. Tiktopulo, V. E. Bychkova, J. Rička, and O. B. Ptitsyn, Macromolecules **27**, 2879 (1994).
[14] C. Wu and S. Zhou, Macromolecules **28**, 8381 (1995).
[15] E. I. Tiktopulo *et al.*, Macromolecules **28**, 7519 (1995).
[16] B. Chu, Q. Ying, and A. Y. Grosberg, Macromolecules **28**, 180 (1995).
[17] J. Naghizadeh and J. Kovac, Phys. Rev. B **34**, 1984 (1986).
[18] P. Grassberger and R. Hegger, J. Phys.: Condens. Matter **7**, 3089 (1995).
[19] Y. A. Kuznetsov, E. G. Timoshenko, and K. A. Dawson, J. Chem. Phys. **103**, 4807 (1995).
[20] M. Wittkop, S. Kreitmeier, and D. Göritz, J. Chem. Phys. **104**, 3373 (1996).
[21] K. Binder and W. Paul, J. Polym. Sci., Part B: Polym. Phys. **35**, 1 (1997).
[22] Y. Zhou, M. Karplus, J. M. Wichert, and C. K. Hall, J. Chem. Phys. **107**, 10691 (1997).
[23] H. Schild and D. Tirrell, Polym. Prepr. (Am. Chem. Soc. Div. Polym. Chem.) **30**, 350 (1989).
[24] H. Schild and D. Tirrell, Langmuir **7**, 665 (1991).
[25] G. Karlström, A. Celsson, and B. Lindman, J. Phys. Chem. **94**, 5005 (1990).
[26] R. Walter, J. Rička, C. Quellet, R. Nyffenegger, and T. Binkert, Macromolecules **29**, 4019 (1996).
[27] J. Rička, M. Meewes, R. Nyffenegger, and T. Binkert, Phys. Rev. Lett. **65**, 657 (1990).
[28] M. Meewes, J. Rička, M. d. Silva, R. Nyffenegger, and T. Binkert, Macromolecules **24**, 5811 (1991).
[29] K. Zhang, G. Karlstrom, and B. Lindman, J. Phys. Chem. **98**, 4411 (1994).
[30] A. Moskalenko and K. Dawson, J. Chem. Phys. **102**, 8208 (1995).
[31] E. Kokufuta, Y.-Q. Zhang, T. Tanaka, and A. Mamada, Macromolecules **26**, 1053 (1993).
[32] Y. S. Kang and L. Kevan, J. Phys. Chem. **98**, 7624 (1994).
[33] D. M. Bloor, J. F. Holzwarth, and E. Wyn-Jones, Langmuir **11**, 2312 (1995).
[34] D. M. Bloor *et al.*, Langmuir **11**, 3395 (1995).
[35] C. Holmberg, S. Nilsson, and L.-O. Sundelöf, Langmuir **13**, 1392 (1997).
[36] P. W. Zhu and D. H. Napper, Langmuir **12**, 5992 (1996).
[37] G. G. Pereira, D. R. M. Williams, and D. H. Napper, Langmuir **15**, 906 (1999).
[38] B. Cabane, J. Phys. Chem. **81**, 1639 (1977).
[39] B. Cabane and R. Duplessix, J. Phys. (Paris) **48**, 651 (1987).
[40] D. E. Jennings, Y. A. Kuznetsov, E. G. Timoshenko, and K. A. Dawson, J. Chem. Phys. **108**, 1702 (1998).
[41] D. E. Jennings, Y. A. Kuznetsov, E. G. Timoshenko, and K. A. Dawson, Nuovo Cimento D **20**, 2365 (1998).
[42] M. Schick and W.-H. Shih, Phys. Rev. Lett. **59**, 1205 (1987).
[43] G. Gompper and M. Schick, Phys. Rev. Lett. **62**, 1647 (1989).
[44] G. Gompper and M. Schick, Phys. Rev. B **41**, 9148 (1990).
[45] K. A. Dawson and Z. Kurtović, J. Chem. Phys. **92**, 5473 (1990).
[46] J. R. Gunn and K. A. Dawson, J. Chem. Phys. **96**, 3152 (1992).
[47] K. A. Dawson, B. L. Walker, and A. Berera, Physica A **165**, 320 (1990).
[48] G. Gompper and M. Schick, *Phase Transitions and Critical Phenomena* (Academic, London, 1994), Vol. 16, Chap. Self-Assembling Amphiphilic Systems.
[49] D. Stauffer *et al.*, J. Chem. Phys. **100**, 6934 (1994).
[50] Y. J. Nikas and D. Blankschtein, Langmuir **10**, 3513 (1994).
[51] B. Jönsson, B. Lindman, K. Holmberg, and B. Kronberg, *Surfactants and Polymers in Aqueous Solution* (Wiley, New York, 1998), Chap. 11, pp. 219–224.
[52] Y. A. Kuznetsov, E. G. Timoshenko, and K. A. Dawson, J. Chem. Phys. **104**, 336 (1196).